Fuzzy descriptor tracking control with guaranteed L∞ error-bound for robot manipulators

Tran Anh-Tu Nguyen, Antoine Dequidt, van Anh Nguyen Thi, Laurent Vermeiren, Michel Dambrine

Fuzzy Descriptor Tracking Control with Guaranteed L∞ Error-Bound for Robot Manipulators

Article *in* Transactions of the Institute of Measurement and Control · November 2020

DOI: 10.1177/0142331220979262

5 authors, including:

Anh-Tu Nguyen
Université Polytechnique Hauts-de-France
140 PUBLICATIONS **2,084** CITATIONS
SEE PROFILE

Antoine Dequidt
Université Polytechnique Hauts-de-France
77 PUBLICATIONS **470** CITATIONS
SEE PROFILE

Laurent Vermeiren
Université Polytechnique Hauts-de-France
82 PUBLICATIONS **1,776** CITATIONS
SEE PROFILE

Michel Dambrine
Université Polytechnique Hauts-de-France
151 PUBLICATIONS **4,316** CITATIONS
SEE PROFILE

Fuzzy Descriptor Tracking Control with Guaranteed $\mathcal{L}_\infty$ Error-Bound for Robot Manipulators

Anh-Tu Nguyen*, Antoine Dequidt, Van-Anh Nguyen, Laurent Vermeiren, Michel Dambrine
LAMIH laboratory UMR CNRS 8201, Univ. Polytechnique Hauts-de-France, Valenciennes, France
*Corresponding author (email: tnguyen@uphf.fr)

Abstract

This paper is concerned with the nonlinear tracking control design for robot manipulators. In spite of the rich literature in the field, the problem has not yet been addressed adequately due to the lack of an effective control design. Using a descriptor fuzzy model-based framework, we propose a new approach to design a feedback-feedforward control scheme for robot manipulators in a general form. The goal is to guarantee a small level of an $\mathcal{L}_\infty-$gain specification to improve the tracking performance while significantly reducing the numerical complexity for real-time implementation. Based on Lyapunov stability arguments, the control design is formulated as a convex optimization problem involving linear matrix inequalities. Numerical experiments performed with a high-fidelity manipulator benchmark model, embedded in the Simscape Multibody™ environment, demonstrate the effectiveness of the proposed control solution over existing standard approaches.

Index Terms

Robot manipulators, fuzzy control, tracking control, Lyapunov stability, $\mathcal{L}_\infty$ performance, linear matrix inequality.

I. Introduction

Nowadays, robot manipulators are widely used in all areas of industry for process automation such as material handling, welding, painting, cutting, grinding, etc. These industrial robots have several advantages, including high speed, compactness, accuracy and reliability. For applications such as arc welding, laser cutting or machining, one of the most important tasks is to obtain a satisfactory tracking performance of predefined reference trajectories (Dawson et al. 2003). It is well-known that tracking control is more challenging than stabilization or regulation problems. First, the tracking controller must drive the system output toward a desired reference with specified closed-loop properties. Second, the stabilization/regulation issue can be viewed as a special case of tracking control, for which the desired trajectory is constant in time. Moreover, tracking control of robot manipulators is challenging due to complex nonlinearities, coupling dynamics effects, unknown disturbances, and modeling uncertainties (Baek et al. 2016, Sun, Zhang, Li & Zhang 2019, Li & Huang 2020).

Up to now, numerous tracking control approaches have been proposed for robot manipulators, including proportional-integral-derivative (PID) control (Jafarov et al. 2005, Arteaga-Pérez 2019, Pan et al. 2019), fuzzy logic control (Marwan et al. 2013, Gaidhane et al. 2019), observer-based backstepping control (Sahu et al. 2019), sliding mode control (Baek et al. 2016, de Jesús Rubio 2017, Zhang, Liu, Wang & Xia 2018), $\mathcal{H}_\infty$ control (Makarov et al. 2016), fault-tolerant tracking control (Van et al. 2016, Meng et al. 2020), adaptive control (Nojavanzadeh & Badamchizadeh 2016, Yang et al. 2018, Zhang, Chen, Li & Zhang 2017, Sun, Su, Xia & Nguyen 2019), neural networks control (Zhang et al. 2016, Zhang, Zheng, Yu, Li & Yu 2017, Jin et al. 2018, Zhang, Dong, Ouyang, Yin & Peng 2018), boundary vibration control (He et al. 2018), reinforcement learning control (Ouyang et al. 2017), Riccati equation-based approach (Nasiri et al. 2020), etc. Despite great theoretical advances in robotics control, single-axis PID control still remains the predominant method for industrial robot manipulators due to its simple structure, easy tuning and convenient implementation (Paccot et al. 2009). However, without taking into account the coupling between different robot joints, linear PID control may lead to a significant loss of performance even closed-loop instability under various practical configurations (Vermeiren et al. 2012). Computed torque control (CTC) technique has been widely applied in robotics (Dawson et al. 2003, Song et al. 2005, Buondonno & De Luca 2016, Paccot et al. 2009). An alternative solution to improve the tracking performance is to combine a feedforward action based on the manipulator dynamics together

with a feedback control action. However, the resulting feedback-feedforward control structures suffer the robustness issue with respect to the modeling uncertainty and the external disturbance forces. To overcome this major drawback, fuzzy control has been proposed for the robot tracking problem (Tseng et al. 2001, Vermeiren et al. 2012, Nguyen, Taniguchi, Eciolaza, Campos, Palhares & Sugeno 2019, Nguyen, Nguyen, Dequidt, Vermeiren & Dambrine 2019). However, the control design complexity and the tracking precision may be further improved for generic robot manipulators.

Over the past decades, fuzzy tracking control has been actively investigated for nonlinear systems (Nguyen, Taniguchi, Eciolaza, Campos, Palhares & Sugeno 2019). The fruitful results can be classified into two major categories: fuzzy adaptive control scheme (Chen et al. 2007, Zhou et al. 2011, Wang et al. 2016, Li et al. 2017) and fuzzy model-based control scheme (Tseng et al. 2001, Jia et al. 2009, Zhang et al. 2013, Pan et al. 2020, Nguyen, Rath, Guerra, Palhares & Zhang 2020). Despite a great theoretical interest, fuzzy adaptive control usually requires *online* complex adaptation laws to deal with unknown parameters and nonlinearities, which may induce real-time difficulties. Since robot modeling has been well-established (Dawson et al. 2003), fuzzy model-based control approaches would be more appropriate for high-speed motion tracking of industrial manipulators as recently shown in (Nguyen, Nguyen, Dequidt, Vermeiren & Dambrine 2019, Jonnalagadda et al. 2020). Note that the existing fuzzy model-based approaches mostly rely on the well-known $\mathcal{H}_\infty$ specification to guarantee the tracking performance which can lead to the following drawbacks, especially for complex industrial manipulators. First, an *explicit* requirement and consideration of a reference model for tracking control design may induce unnecessary numerical complexities. Second, the effects of both known tracking reference and unknown external forces on the tracking error have been treated in the same fashion, *i.e.*, *unknown* disturbances. This may result in conservative control results. Third, the $\mathcal{H}_\infty$ specification represents the energy-to-energy gain of the close-loop system. However, in most of practical situations as robotics control, the disturbances, *e.g.*, friction torques, are rather amplitude-bounded than energy-bounded. Hence, within an $\mathcal{H}_\infty$ control formulation, it is not obvious to characterize the amplitude-bound of the tracking error, which is a crucial tracking performance index.

Motivated by the above practical and theoretical issues in manipulator control, this paper proposes a fuzzy model-based control approach for high-precision and high-speed motion tracking problem of generic robot manipulators. The main contributions of the proposed fuzzy tracking control framework can be summarized as follows.

- We exploit the specific descriptor form of robot manipulators to derive a feedback-feedforward tracking control scheme. The feedforward control action aims at accounting for the effects of known disturbances to improve the tracking performance. Based on a fuzzy descriptor tracking error dynamics and Lyapunov arguments, the feedback control action is designed to guarantee some predefined closed-loop properties. The feedback control design is recast as an optimization problem with linear matrix inequality (LMI) constraints, effectively solved with available numerical solvers (Boyd et al. 1994).
- In contrast to the standard $\mathcal{H}_\infty$ tracking performance, a new $\mathcal{L}_\infty-$gain specification is taken into the control design to guarantee a tracking error-bound as small as possible according to the solvability of the optimization-based control problem. Moreover, the new framework offers a simple and systematic approach not only for the control design but also for the real-time implementation. This feature is particularly interesting for industrial robot applications.
- The effectiveness of the proposed tracking control approach is clearly demonstrated with a high-fidelity manipulator benchmark developed by ABB Robotics (Moberg et al. 2008). A comparative study between different notable tracking control approaches is performed to emphasize the interests of the new control framework.

The paper is organized as follows. The tracking control problem is formulated in Section II. The fuzzy model-based feedback control design is presented in Section III. Section IV provides numerical experiments obtained with a 2-DoF robot benchmark. Concluding remarks are reported in Section V.

Notation. Ω_r denotes the set of numbers $\{1, 2, ..., r\}$. For a matrix X, $X^\top$ denotes its transpose, $X \succ 0$ means that X is positive definite, $\mathrm{He}X = X + X^\top$, and $\lambda_{\min}(X)$, $\lambda_{\max}(X)$ denotes respectively the minimal and maximal eigenvalues of a symmetric matrix X. For a vector $\mathbf{v} \in \mathbb{R}^n$, we denote its 2-norm as $\|\mathbf{v}\| = \sqrt{\mathbf{v}^\top \mathbf{v}}$, and v_i is its ith entry. For a function $f : \mathbb{R} \to \mathbb{R}^n$, its $\mathcal{L}_\infty-$norm is defined as $\|f\|_\infty = \sup_{t\in\mathbb{R}} \|f(t)\|$, and $\mathfrak{B}_\infty$ is the set of bounded functions f. $\mathrm{diag}(X_1, X_2)$ denotes a block-diagonal matrix composed of X_1, X_2. I is the identity matrix of appropriate dimension. $\star$ stands for the terms deduced by symmetry. The argument of a function is omitted when its meaning is clear.

II. Tracking Control Formulation

We first introduce the general model of robot manipulators. Then, the related tracking control problem is formulated.

A. Descriptor Representation of Robot Manipulators

The rigid-body dynamics of an n degrees of freedom (DoF) robot manipulator can be expressed in the joint space as

$$\mathcal{M}(\mathbf{q})\ddot{\mathbf{q}}(t) + \mathcal{N}(\mathbf{q}, \dot{\mathbf{q}})\dot{\mathbf{q}}(t) + \mathcal{G}(\mathbf{q}) = \Gamma(t) + \Gamma_d(t), \tag{1}$$

where $\mathbf{q}(t) \in \mathbb{R}^n$ is the vector of generalized coordinates in joint space, $\Gamma(t) \in \mathbb{R}^n$ is the vector of generalized control forces, $\Gamma_d(t) \in \mathbb{R}^n$ is the vector of external generalized forces applied to the joints, $\mathcal{M}(\mathbf{q}) \in \mathbb{R}^{n\times n}$ is the inertia matrix, $\mathcal{N}(\mathbf{q}, \dot{\mathbf{q}}) \in \mathbb{R}^{n\times n}$ is the Coriolis/centripetal matrix plus the viscous friction coefficients of the joints, and $\mathcal{G}(\mathbf{q}) \in \mathbb{R}^n$ represents the generalized gravity forces. Note that the dynamics (1) can account for many types of robot manipulators (Dawson et al. 2003). Since the vector field $\mathcal{G}(\mathbf{q})$ is smooth, we can then parameterize $\mathcal{G}(\mathbf{q}) = \mathcal{P}(\mathbf{q})\mathbf{q}(t)$. The disturbance $\Gamma_d(t)$ is amplitude-bounded, *i.e.*, $\Gamma_d(t) \in \mathfrak{B}_\infty$. Note that for the proposed fuzzy-model-based control approach, the matrices $\mathcal{M}(\mathbf{q})$, $\mathcal{N}(\mathbf{q}, \dot{\mathbf{q}})$ and $\mathcal{P}(\mathbf{q})\mathbf{q}(t)$ characterizing the robot dynamics are assumed to be known.

Let us denote $\mathbf{x}(t) = \begin{bmatrix}\mathbf{q}^\top(t) & \dot{\mathbf{q}}^\top(t)\end{bmatrix}^\top$, the manipulator dynamics (1) can be rewritten in the following descriptor form:

$$E(\mathbf{x})\dot{\mathbf{x}}(t) = A(\mathbf{x})\mathbf{x}(t) + B(\Gamma(t) + \Gamma_d(t)), \tag{2}$$

where

$$E(\mathbf{x}) = \begin{bmatrix} I & 0 \\ 0 & \mathcal{M}(\mathbf{q}) \end{bmatrix}, \quad A(\mathbf{x}) \quad = \begin{bmatrix} 0 & I \\ -\mathcal{P}(\mathbf{q}) & -\mathcal{N}(\mathbf{q}, \dot{\mathbf{q}}) \end{bmatrix}, \quad B = \begin{bmatrix} 0 \\ I \end{bmatrix}.$$

Note that due to the physical constraints, the state vector $\mathbf{x}(t)$ remains in a bounded set $\mathscr{D}_x$, defined as

$$\mathscr{D}_x = \left\{\mathbf{x} \in \mathbb{R}^{2n} : \; x_{i\min} \le x_i(t) \le x_{i\max}\right\}. \tag{3}$$

The given bounds $x_{i\min}$ and $x_{i\max}$, $i \in \Omega_{2n}$, characterize the workspace and the joint velocity limitations of the manipulator.

B. Feedback-Feedforward Structure for Tracking Control

The reference trajectory of robot manipulators can be completely defined by designers as

$$\mathbf{x}_r(t) = \begin{bmatrix}\mathbf{q}_r^\top(t) & \dot{\mathbf{q}}_r^\top(t)\end{bmatrix}^\top,$$

where $\mathbf{q}_r(t), \dot{\mathbf{q}}_r(t) \in \mathbb{R}^n$ are respectively the reference position and velocity to be followed. For tracking control, we assume that $\mathbf{x}_r$ is sufficiently smooth, *i.e.*, $\mathbf{q}_r(t) \in \mathcal{C}^2$.

We define the tracking error as $\mathbf{e}(t) = \mathbf{x}(t) - \mathbf{x}_r(t)$. Then, the error dynamics can be derived from model (2) as

$$E(\mathbf{x})\dot{\mathbf{e}}(t) = A(\mathbf{x})\mathbf{e}(t) + B(\Gamma(t) + \mathbf{d}(t)) + \mathcal{R}(\mathbf{x}, \mathbf{x}_r, \dot{\mathbf{x}}_r) \tag{4}$$

where $\mathcal{R}(\mathbf{x}, \mathbf{x}_r, \dot{\mathbf{x}}_r) = A(\mathbf{x})\mathbf{x}_r(t) - E(\mathbf{x})\dot{\mathbf{x}}_r(t)$, and $\mathbf{d}(t) = \Gamma_d(t)$. To improve the tracking control performance, the control input $\Gamma(t)$ is decomposed into two parts as

$$\Gamma(t) = \mathbf{u}_{\text{fb}}(t) + \mathbf{u}_{\text{ff}}(t). \tag{5}$$

The feedback control $\mathbf{u}_{\text{fb}}(t)$, specified in Section III, is used to ensure predefined properties of the tracking error dynamics under disturbances and uncertainties. The feedforward control $\mathbf{u}_{\text{ff}}(t)$ accounts for the effects of $\mathbf{x}_r(t)$ on the tracking error $\mathbf{e}(t)$. From (4) and (5), the error dynamics is defined as

$$E(\mathbf{x})\dot{\mathbf{e}}(t) = A(\mathbf{x})\mathbf{e}(t) + B(\mathbf{u}_{\text{fb}}(t) + \mathbf{d}(t)) + \mathcal{Q}(\mathbf{u}_{\text{ff}}, \mathbf{x}, \mathbf{x}_r) \tag{6}$$

where $\mathcal{Q}(\mathbf{u}_{\text{ff}}, \mathbf{x}, \mathbf{x}_r) = B\mathbf{u}_{\text{ff}}(t) + \mathcal{R}(\mathbf{x}, \mathbf{x}_r, \dot{\mathbf{x}}_r)$. Since $\mathbf{x}_r(t)$ and $\dot{\mathbf{x}}_r(t)$ are *known*, $\mathbf{u}_{\text{ff}}(t)$ aims at mitigating the effects of these exogenous signals on the tracking error dynamics, *i.e.*,

$$\mathcal{Q}(\mathbf{u}_{\text{ff}}, \mathbf{x}, \mathbf{x}_r) = B\mathbf{u}_{\text{ff}}(t) - E(\mathbf{x})\dot{\mathbf{x}}_r(t) + A(\mathbf{x})\mathbf{x}_r(t) = 0. \tag{7}$$

Since matrix B is of full column rank, its pseudo-inverse $B^\dagger$ exists and $B^\dagger B = I$. Premultiplying (7) with $B^\dagger$, the feedforward control law is derived as follows:

$$\mathbf{u}_{\text{ff}}(t) = B^\dagger(E(\mathbf{x})\dot{\mathbf{x}}_r(t) - A(\mathbf{x})\mathbf{x}_r(t)). \tag{8}$$

From (6) and (8), the tracking error dynamics is rewritten as

$$E(\mathbf{x})\dot{\mathbf{e}}(t) = A(\mathbf{x})\mathbf{e}(t) + B(\mathbf{u}_{\text{fb}}(t) + \mathbf{d}(t)). \tag{9}$$

We are now in the position to formulate the control problem related to the closed-loop tracking error system (9).

Problem 1. Determine a feedback control law $\mathbf{u}_{\text{fb}}(t)$ such that the error dynamics (9) satisfies the following properties.

(P1) For zero-disturbance system, *i.e.*, $\mathbf{d}(t) = 0$, for $\forall t \geq 0$, the zero solution of system (9) is *exponentially* stable with a predefined decay rate $\alpha > 0$.

(P2) The closed-loop system (9) is input-to-state stable with respect to the disturbance $\mathbf{d}(t)$.

(P3) For a zero initial tracking error, *i.e.*, $\mathbf{e}(0) = 0$, we have

$$\|\mathbf{e}(t)\| \leq \gamma \|\mathbf{d}(t)\|_\infty, \quad t \geq 0,$$

for some positive scalar γ.

The tracking error dynamics (9) verifying the properties (P1)–(P3) is said to be uniformly $\mathcal{L}_\infty-$stable with a performance level γ. A similar concept of $\mathcal{L}_\infty-$stablity can be found in (Nguyen, Guerra, Sentouh & Zhang 2019, Nguyen et al. 2021). Hereafter, we provide a numerically tractable solution for the above $\mathcal{L}_\infty-$gain tracking control problem.

III. $\mathcal{L}_\infty$ Fuzzy Descriptor Control Design

This section first transforms the error tracking dynamics into an exact fuzzy descriptor form. Then, an LMI-based solution is proposed for Problem 1. Finally, based on a robust control scheme, complexity-reduced feedback control law is proposed.

A. Fuzzy Descriptor Representation of the Error Dynamics

For control design, system (9) is transformed into its *equivalent* fuzzy representation using the sector nonlinearity approach (Tanaka & Wang 2004, Chapter 2). To this end, we first determine the vector of premise variables $\mathbf{z}(t) = \begin{bmatrix} z_1(t) & \dots & z_{p_e+p}(t) \end{bmatrix}$, containing p_e and p linearly *independent* nonlinearities in $E(\mathbf{x})$ and $A(\mathbf{x})$, respectively. Since $\mathbf{x}(t) \in \mathscr{D}_x$, it follows that $z_i(t) \in \begin{bmatrix} z_{i\min}, z_{i\max} \end{bmatrix}$, where $z_{i\min}$ and $z_{i\max}$, for $\forall i \in \Omega_{p_e+p}$, are easily computed from the bounds given in (3). Moreover, each premise variable can be *equivalently* rewritten as $z_i(t) = \psi_0^i(z_i) z_{i\min} + \psi_1^i(z_i) z_{i\max}$, where

$$\psi_0^i(z_i) = \frac{z_{i\max} - z_i(t)}{z_{i\max} - z_{i\min}}, \quad \psi_1^i(z_i) = 1 - \psi_0^i(z_i), \quad i \in \Omega_{p_e+p}.$$

As a consequence, the error dynamics (9) can be represented in the following fuzzy descriptor form (Taniguchi et al. 2000):

$$\sum_{k=1}^{r_e} v_k(\mathbf{z}) E_k \dot{\mathbf{e}}(t) = \sum_{i=1}^{r} h_i(\mathbf{z}) A_i \mathbf{e}(t) + B(\mathbf{u}_{\text{fb}}(t) + \mathbf{d}(t)). \tag{10}$$

The membership functions (MFs) are defined as follows (Tanaka & Wang 2004):

$$v_k(\mathbf{z}) = \prod_{j=1}^{p_e} \psi_{k_j}^j(z_j), \quad h_i(\mathbf{z}) = \prod_{j=p_e+1}^{p_e+p} \psi_{i_j}^j(z_j),$$

where $k_j, i_j \in \{0, 1\}$, $(k, i) \in \Omega_{r_e} \times \Omega_r$, $r_e = 2^{p_e}$ and $r = 2^p$. Note that $E_k = E(\mathbf{x})|_{v_k(\mathbf{z})=1}$, $A_i = A(\mathbf{x})|_{h_i(\mathbf{z})=1}$ and the MFs satisfy the following convex sum property:

$$\begin{aligned} &\sum_{k=1}^{r_e} v_k(\mathbf{z}) = 1, \quad v_k(\mathbf{z}) \geq 0, \quad k \in \Omega_{r_e}, \\ &\sum_{i=1}^{r} h_i(\mathbf{z}) = 1, \quad h_i(\mathbf{z}) \geq 0, \quad i \in \Omega_r. \end{aligned} \tag{11}$$

Remark 1. Due to the nonsingularity of $E(\mathbf{x})$, a standard state-space model can be directly recovered from the descriptor form (9) as $\dot{\mathbf{e}}(t) = E(\mathbf{x})^{-1}A(\mathbf{x})\mathbf{e}(t) + E(\mathbf{x})^{-1}B(\mathbf{u}_{\text{fb}}(t) + \mathbf{d}(t))$. However, such a representation significantly complexifies the nonlinear control design since a large number of new premise variables is introduced, *e.g.*, the input matrix $E(\mathbf{x})^{-1}B$ is not anymore constant. Keeping the descriptor form (9) reduces the number of linear submodels of the fuzzy model (10), thus the number of design conditions. This allows reducing the computational burden, the control structure complexity and also the design conservatism (Taniguchi et al. 2000).

Let us define $\bar{\mathbf{e}}(t) = \begin{bmatrix}\mathbf{e}^\top(t) & \dot{\mathbf{e}}^\top(t)\end{bmatrix}^\top$. Then, the fuzzy descriptor system (10) can be rewritten as

$$\bar{E}\dot{\bar{\mathbf{e}}}(t) = \sum_{i=1}^{r}\sum_{k=1}^{r_e} h_i(\mathbf{z})v_k(\mathbf{z})\bar{A}_{ik}\bar{\mathbf{e}}(t) + \bar{B}(\mathbf{u}_{\text{fb}}(t) + \mathbf{d}(t)), \tag{12}$$

where

$$\bar{E} = \begin{bmatrix} I & 0 \\ 0 & 0 \end{bmatrix}, \quad \bar{B} = \begin{bmatrix} 0 \\ B \end{bmatrix}, \quad \bar{A}_{ik} = \begin{bmatrix} 0 & I \\ A_i & -E_k \end{bmatrix}. \tag{13}$$

For the control design of system (12), we consider the nonlinear feedback control law of the form

$$\mathbf{u}_{\text{fb}}(t) = -\sum_{i=1}^{r}\sum_{k=1}^{r_e} h_i(\mathbf{z})v_k(\mathbf{z})K_{ik}\mathbf{e}(t), \tag{14}$$

where the feedback gains $K_{ik} \in \mathbb{R}^{n\times 2n}$ are to be designed. From (10) and (14), the closed-loop error dynamics can be expressed on the following descriptor fuzzy form:

$$\bar{E}\dot{\bar{\mathbf{e}}}(t) = \sum_{i=1}^{r}\sum_{k=1}^{r_e} h_i(\mathbf{z})v_k(\mathbf{z})(\bar{A}_{ik} - \bar{B}\bar{K}_{ik})\bar{\mathbf{e}}(t) + \bar{B}\mathbf{d}(t), \tag{15}$$

where $\bar{K}_{ik} = \begin{bmatrix} K_{ik} & 0 \end{bmatrix}$. This paper proposes two procedures to design the feedback control law (14) with different degrees of numerical complexity such that the closed-loop specifications as defined in Problem 1 are satisfied for system (15).

B. LMI-Based Feedback Control Design

The following result provides an LMI-based conditions to design a feedback control law (14) solving Problem 1.

Theorem 1. Consider the tracking error dynamics (9). Given a positive decay rate α, assume that there exist a positive definite matrix $P \in \mathbb{R}^{2n\times 2n}$, matrices $Q_i \in \mathbb{R}^{2n\times 2n}$, $R_i \in \mathbb{R}^{2n\times 2n}$, $M_{ik} \in \mathbb{R}^{n\times 2n}$, for $\forall (i,k) \in \Omega_r \times \Omega_{r_e}$, and a positive scalar ν, solutions of the following optimization problem:

$$\texttt{minimize} \quad \nu \tag{16}$$

subject to

$$\begin{bmatrix} P & \star \\ P & \nu I \end{bmatrix} \succeq 0, \tag{17}$$

$$\Xi_{ik} \prec 0, \quad \forall (i,k) \in \Omega_r \times \Omega_{r_e}, \tag{18}$$

where

$$\Xi_{ik} = \text{He}\begin{bmatrix} \alpha P + Q_i & R_i & 0 \\ A_i P - BM_{ik} - E_k Q_i & -E_k R_i & B \\ 0 & 0 & -\alpha I \end{bmatrix}.$$

Then, the feedback law (14) with the gains $K_{ik} = M_{ik}P^{-1}$, for $(i,k) \in \Omega_r \times \Omega_{r_e}$, is such that the properties given in Problem 1 are satisfied with the guaranteed $\mathcal{L}_\infty-$gain $\gamma = \sqrt{\nu}$.

Proof. Multiplying inequality (18) by $h_i(\mathbf{z})v_k(\mathbf{z})$ and summing up for $i \in \Omega_r$ and $k \in \Omega_{r_e}$, it follows that

$$\sum_{i=1}^{r}\sum_{k=1}^{r_e} h_i(\mathbf{z})v_k(\mathbf{z})\text{He}(E_k R_i) \succ 0,$$

which can be rewritten as

$$\mathrm{He}\left(\left(\sum_{k=1}^{r_e} v_k(\mathbf{z})E_k\right)\left(\sum_{i=1}^{r} h_i(\mathbf{z})R_i\right)\right) \succ 0. \tag{19}$$

Inequality (19) implies the regularity of $\sum_{i=1}^{r} h_i(\mathbf{z})R_i$. This allows us to define a Lyapunov candidate function of the form

$$\mathcal{V}(\bar{\mathbf{e}}) = \bar{\mathbf{e}}^\top \bar{E}\left(\sum_{i=1}^{r} h_i(\mathbf{z})\bar{P}_i\right)^{-1}\bar{\mathbf{e}}, \quad \bar{P}_i = \begin{bmatrix} P & 0 \\ Q_i & R_i \end{bmatrix}. \tag{20}$$

Remark that

$$\bar{E}\left(\sum_{i=1}^{r} h_i(\mathbf{z})\bar{P}_i\right)^{-1} = \left(\sum_{i=1}^{r} h_i(\mathbf{z})\bar{P}_i\right)^{-1}\bar{E} = \begin{bmatrix} P^{-1} & 0 \\ 0 & 0 \end{bmatrix}.$$

Then, $\mathcal{V}(\bar{\mathbf{e}}(t))$, defined in (20), can be rewritten as $\mathcal{V}(\bar{\mathbf{e}}(t)) = \mathcal{V}(\mathbf{e}(t)) = \mathbf{e}^\top(t)P^{-1}\mathbf{e}(t)$, which is a positive definite function of $\mathbf{e}(t)$. We denote $\hat{\mathbf{e}}(t) = \left(\sum_{i=1}^{r} h_i(\mathbf{z})\bar{P}_i\right)^{-1}\bar{\mathbf{e}}(t)$. The time-derivative of $\mathcal{V}(\bar{\mathbf{e}}(t))$ along the trajectory of system (15) can be expressed as

$$\begin{aligned}\dot{\mathcal{V}}(\bar{\mathbf{e}}(t)) &= \mathrm{He}\left(\left[\mathcal{A}_z\bar{\mathbf{e}}(t) + \bar{B}\mathbf{d}(t)\right]^\top \bar{P}_h\bar{\mathbf{e}}(t)\right) \\ &= \mathrm{He}\left\{\left[\mathcal{A}_z\bar{P}_h\hat{\mathbf{e}}(t) + \bar{B}\mathbf{d}(t)\right]^\top \hat{\mathbf{e}}(t)\right\},\end{aligned} \tag{21}$$

where $\mathcal{A}_z = \sum_{i=1}^{r}\sum_{k=1}^{r_e} h_i(\mathbf{z})v_k(\mathbf{z})(\bar{A}_{ik} - \bar{B}\bar{K}_{ik})$ and $\bar{P}_h = \sum_{i=1}^{r} h_i(\mathbf{z})\bar{P}_i$. From the matrix definition (13), the expressions of $\mathcal{V}(\bar{\mathbf{e}}(t))$ in (20) and of $\dot{\mathcal{V}}(\bar{\mathbf{e}}(t))$ in (21), the following relation can be obtained after simple matrix multiplications:

$$\dot{\mathcal{V}}(\bar{\mathbf{e}}(t)) + 2\alpha\left(\mathcal{V}(\bar{\mathbf{e}}(t)) - \mathbf{d}^\top(t)\mathbf{d}(t)\right) = \xi^\top(t)\Xi_{hv}\xi(t), \tag{22}$$

with $\xi = \begin{bmatrix}\hat{\mathbf{e}}^\top & \mathbf{d}^\top\end{bmatrix}^\top$ and $\Xi_{hv} = \sum_{i=1}^{r}\sum_{k=1}^{r_e} h_i(\mathbf{z})v_k(\mathbf{z})\Xi_{ik}$. Using the convexity property (11) of the membership functions, it follows from (18) that $\Xi_{hv} \prec 0$. Combining this with (22), it follows that

$$\begin{aligned}\dot{\mathcal{V}}(\bar{\mathbf{e}}(\tau)) &\leq -2\alpha(\mathcal{V}(\bar{\mathbf{e}}(\tau)) - \|\mathbf{d}(\tau)\|^2) \\ &\leq -2\alpha(\mathcal{V}(\bar{\mathbf{e}}(\tau)) - \|\mathbf{d}(\tau)\|_\infty^2), \quad \forall\tau > 0.\end{aligned} \tag{23}$$

Multiplying both sides of inequality (23) by $e^{2\alpha t}$, then integrating the result over $[t_0, t]$, we get

$$\begin{aligned}e^{2\alpha t}\mathcal{V}(\bar{\mathbf{e}}(t)) &\leq e^{2\alpha t_0}\mathcal{V}(\bar{\mathbf{e}}(t_0)) + 2\alpha\|\mathbf{d}(t)\|_\infty^2\int_{t_0}^{t} e^{2\alpha\tau}d\tau \\ &= e^{2\alpha t_0}\mathcal{V}(\bar{\mathbf{e}}(t_0)) + \|\mathbf{d}(t)\|_\infty^2(e^{2\alpha t} - e^{2\alpha t_0}).\end{aligned} \tag{24}$$

It follows from (24) that

$$\begin{aligned}\mathcal{V}(\bar{\mathbf{e}}(t)) &\leq e^{-2\alpha(t-t_0)}\mathcal{V}(\bar{\mathbf{e}}(t_0)) + \|\mathbf{d}(t)\|_\infty^2\left(1 - e^{-2\alpha(t-t_0)}\right) \\ &\leq e^{-2\alpha(t-t_0)}\mathcal{V}(\bar{\mathbf{e}}(t_0)) + \|\mathbf{d}(t)\|_\infty^2.\end{aligned} \tag{25}$$

By Schur complement lemma (Boyd et al. 1994), inequality (17) is equivalent to $P^{-1} \succeq \nu^{-1}I$. Then, denote $\sigma_M = \lambda_{\max}(P^{-1})$, the Lyapunov function $\mathcal{V}(\bar{\mathbf{e}})$ satisfies

$$\nu^{-1}\|\mathbf{e}(t)\|^2 \leq \mathcal{V}(\bar{\mathbf{e}}(t)) \leq \sigma_M\|\mathbf{e}(t)\|^2. \tag{26}$$

It follows from (25) and (26) that

$$\|\mathbf{e}(t)\|^2 \leq \nu\sigma_M e^{-2\alpha(t-t_0)}\|\mathbf{e}(t_0)\|^2 + \nu\|\mathbf{d}(t)\|_\infty^2,$$

which, in turn, implies that

$$\|\mathbf{e}(t)\| \leq \sqrt{\nu\sigma_M}e^{-\alpha(t-t_0)}\|\mathbf{e}(t_0)\| + \sqrt{\nu}\|\mathbf{d}(t)\|_\infty. \tag{27}$$

Inequality (27) guarantees the closed-loop properties (P1), (P2) and (P3) with $\gamma = \sqrt{\nu}$, defined in Problem 1. □

Remark 2. For any initial condition $\mathbf{e}(t_0)$ and for $\forall \mathbf{d}(t) \in \mathfrak{B}_\infty$, it follows from (27) that

$$\limsup_{t\to\infty} \|\mathbf{e}(t)\| \leq \gamma \|\mathbf{d}(t)\|_\infty. \tag{28}$$

It is clear from (28) that minimizing γ leads to a minimized value of $\mathbf{e}(t)$, thus a better tracking performance. Moreover, if the optimization problem (16) in Theorem 1 is feasible with an *arbitrarily* small γ, then the tracking error is arbitrarily small.

C. Reduced-Complexity Fuzzy Tracking Control

Theoretically, the design conditions in Theorem 1 can be applied to any robot manipulators whose dynamics can be described by (1). However, from a practical viewpoint, these conditions may lead to a major numerical limitation. Indeed, the complexity of the fuzzy model (10) is represented by the integers r and r_e, which *exponentially* grow in function of the number of premise variables in $A(\mathbf{x})$ and $E(\mathbf{x})$ of system (2). Hence, for complex manipulators with high degrees of freedom n, the nonlinear feedback law (14) may be impractical due to the limited computational resources of embedded systems. In such situations, an effective reduced-complexity control approach is required to design the nonlinear controller (14). In particular, reduced-complexity feedback controller is still able to guarantee the closed-loop properties defined in Problem 1. For this purpose, we rewrite some premise variables as follows (Nguyen, Coutinho, Guerra, Palhares & Pan 2020):

$$z_j(t) = z_{jm} + \delta_j(t) z_{jr}, \quad \delta_j(t) \in [-1,\ 1], \tag{29}$$

with $z_{jm} = \frac{1}{2}(z_{j\max} + z_{j\min})$, $z_{jr} = \frac{1}{2}(z_{j\max} - z_{j\min})$, for some $j \in \Omega_{p_e+p}$. Substituting (29) into (9), then applying the sector nonlinearity approach described in Section III-A, we can obtain the following fuzzy system:

$$\sum_{k=1}^{r_e^*} v_k(\mathbf{z}) \hat{E}_k \dot{\mathbf{e}}(t) = \sum_{i=1}^{r^*} h_i(\mathbf{z}) \hat{A}_i \mathbf{e}(t) + B(\mathbf{u}_{\text{fb}}(t) + \mathbf{d}(t)) \tag{30}$$

where $\hat{E}_k = E_k^* + \Delta E_k(t)$, $k \in \Omega_{r_e^*}$, with $r_e^* < r_e$, and $\hat{A}_i = A_i^* + \Delta A_i(t)$, $i \in \Omega_{r^*}$, with $r^* < r$. Note that the time-varying matrices $\Delta E_k(t)$ and $\Delta A_i(t)$ can be further parameterized as

$$\Delta E_k(t) = H_e^\top \Delta_e(t) W_{ek}, \quad \Delta A_i(t) = H_a^\top \Delta_a(t) W_{ai},$$

for $\forall (k,i) \in \Omega_{r_e^*} \times \Omega_{r^*}$. The constant matrices of adequate dimensions H_e, H_a, W_{ek}, W_{ai} are constructed from z_{jr} in (29) whereas matrices $\Delta_\ell(t)$, $\ell \in \{e, a\}$, are obtained from the uncertain terms $\delta_j(t)$. Note also that $\Delta_\ell^\top(t)\Delta_\ell(t) \preceq I$, for $\ell \in \{e, a\}$. The obtention of (30) from the nonlinear descriptor system (2) is further illustrated in Section IV-B.

Remark 3. The numerical complexity of system (30), represented by r_e^* and r^*, *exponentially* decreases with respect to the number of the premise variables considered as uncertain terms shown in (29). However, a large number of uncertain terms may introduce more conservatism to the control design of system (30). Note that any time-varying premise variable $z_j(t)$, for $j \in \Omega_{p_e+p}$, can be represented in the form (29). However, in this paper we propose, as far as possible, to exploit the relation (29) to deal with the premise variables depending on the angular velocities. Then, the membership functions of the descriptor fuzzy systems can be constructed with premise variables only depending on the joint positions. These latter can be easily measured with low-cow position sensors. This fact would be useful for the development of a robust fuzzy output tracking control of robot manipulators without requiring velocity sensors.

The following theorem provides an LMI-based solution to design a reduced-complexity feedback control law

$$\mathbf{u}_{\text{fb}}(t) = -\sum_{i=1}^{r^*} \sum_{k=1}^{r_e^*} h_i(\mathbf{z}) v_k(\mathbf{z}) K_{ik}^* \mathbf{e}(t), \tag{31}$$

such that the uncertain fuzzy system (30) satisfies the closed-loop properties specified in Problem 1.

Theorem 2. Consider the tracking error dynamics (30). Given a positive decay rate α, assume that there exist a positive definite matrix $P \in \mathbb{R}^{2n\times 2n}$, matrices $Q_i \in \mathbb{R}^{2n\times 2n}$, $R_i \in \mathbb{R}^{2n\times 2n}$, $M_{ik} \in \mathbb{R}^{n\times 2n}$, and positive scalars ν, ϕ^a_{ik}, ϕ^e_{ik}, for $\forall (i,k) \in \Omega_{r^*} \times \Omega_{r^*_e}$, solutions of the following optimization problem:

$$\texttt{minimize} \quad \nu \tag{32}$$

subject to (17) and

$$\begin{bmatrix} \Xi^*_{ik} & \star & \star \\ \mathcal{S}_{ik}\mathcal{H} & -\mathcal{S}_{ik} & \star \\ \mathcal{W}_{ik} & 0 & -\mathcal{S}_{ik} \end{bmatrix} \prec 0, \quad \forall (i,k) \in \Omega_{r^*} \times \Omega_{r^*_e}, \tag{33}$$

where $\mathcal{S}_{ik} = \mathrm{diag}(\phi^a_{ik} I, \phi^e_{ik} I)$ and

$$\Xi^*_{ik} = \mathrm{He}\begin{bmatrix} \alpha P + Q_i & R_i & 0 \\ A_i^* P - B M_{ik} - E_k^* Q_i & -E_k^* R_i & B \\ 0 & 0 & -\alpha I \end{bmatrix},$$

$$\mathcal{W}_{ik} = \begin{bmatrix} W_{ai} P & 0 & 0 \\ -W_{ek} Q_i & -W_{ek} R_i & 0 \end{bmatrix}, \ \mathcal{H} = \begin{bmatrix} 0 & H_a & 0 \\ 0 & H_e & 0 \end{bmatrix}.$$

Then, the reduced-complexity controller (31) with the gains $K^*_{ik} = M_{ik} P^{-1}$, for $(i,k) \in \Omega_{r^*} \times \Omega_{r^*_e}$, is such that the properties defined in Problem 1 are satisfied with the guaranteed $\mathcal{L}_\infty-$gain $\gamma = \sqrt{\nu}$.

Proof. Multiplying (33) with $h_i(\mathbf{z}) v_k(\mathbf{z}) \geq 0$ and summing up for all $(i,k) \in \Omega_{r^*} \times \Omega_{r^*_e}$, it follows that

$$\begin{bmatrix} \Xi^*_{hv} & \star & \star \\ \mathcal{S}_{hv}\mathcal{H} & -\mathcal{S}_{hv} & \star \\ \mathcal{W}_{hv} & 0 & -\mathcal{S}_{hv} \end{bmatrix} \prec 0, \tag{34}$$

where $\Pi_{hv} = \sum_{i=1}^{r^*} \sum_{k=1}^{r^*_e} h_i(\mathbf{z}) v_k(\mathbf{z}) \Pi_{ik}$, with $\Pi \in \{\Xi^*, \mathcal{S}, \mathcal{W}\}$. Applying the Schur complement lemma, we can prove that (34) is equivalent to

$$\Xi^*_{hv} + \mathcal{H}^\top \mathcal{S}_{hv} \mathcal{H} + \mathcal{W}_{hv}^\top \mathcal{S}_{hv}^{-1} \mathcal{W}_{hv} \prec 0. \tag{35}$$

Denote $\Delta(t) = \mathrm{diag}(\Delta_a(t), \Delta_e(t))$. Since $\Delta^\top(t)\Delta(t) \preceq I$, using the following matrix fact:

$$\mathrm{He}(\mathbf{X}^\top \mathbf{Y}) \preceq \mathbf{X}^\top \mathbf{S} \mathbf{X} + \mathbf{Y}^\top \mathbf{S}^{-1} \mathbf{Y},$$

with $\mathbf{S} = \mathcal{S}_{hv}$, $\mathbf{X} = \mathcal{H}$ and $\mathbf{Y} = \Delta(t)\mathcal{W}_{hv}$, it follows from (35) that

$$\Xi^*_{hv} + \mathrm{He}(\mathcal{H}^\top \Delta(t) \mathcal{W}_{hv}) \prec 0. \tag{36}$$

Consider a Lyapunov candidate function of the form (20) with $r = r^*$. Then, following similar arguments as in the proof of Theorem 1 and from (36), it can be shown that

$$\dot{\mathcal{V}}(\bar{\mathbf{e}}(t)) + 2\alpha \mathcal{V}(\bar{\mathbf{e}}(t)) - 2\alpha\nu \mathbf{d}^\top(t)\mathbf{d}(t) = \xi^\top(t) \Sigma_{hv} \xi(t) < 0,$$

with $\Sigma_{hv} = \Xi^*_{hv} + \mathrm{He}(\mathcal{H}^\top \Delta(t) \mathcal{W}_{hv})$. The guarantee of properties (P1), (P2) and (P3) in Problem 1 with respect to system (30) can be proved as in the proof of Theorem 1. □

Remark 4. A decay rate performance is incorporated in the Lyapunov stability conditions of Theorems 1 and 2 to improve the tracking performance. A large value of the decay rate α leads to a quick error convergence (Tanaka & Wang 2004). However, this may induce aggressive closed-loop behaviors. The tuning of the positive decay rate α can be easily performed using error-and-trial method to obtain a satisfactory tracking control performance in practice.

Remark 5. The control design in Theorem 1 (respectively Theorem 2) is recast as an optimization problem (16) (respectively (32)) under LMI constraints. Such convex optimization problems can be effectively solved with standard numerical solvers

(Boyd et al. 1994). In this paper, the feedback gains of the tracking fuzzy controllers (14) and (31) are computed using YALMIP toolbox and SDPT3 solver (Löfberg 2004).

Remark 6. Solving the optimization problems in Theorems 1 and 2 may yield excessively high feedback gains, which are impractical for real-world applications. To prevent this practical issue, the following LMI constraints can be incorporated in these convex optimization problems:

$$P \succeq \mu I, \quad \tau \leq \varepsilon\mu, \tag{37}$$

$$\begin{bmatrix} \tau I & M_{ik}^\top \\ M_{ik} & \tau I \end{bmatrix} \succeq 0, \quad \forall (i,k) \in \Omega_r \times \Omega_{r_e}, \tag{38}$$

where μ, τ are additional scalar decision variables, and ε is a given Euclidean norm-bound of the matrix gains K_{ik}. Indeed, by Schur complement, inequality (38) is equivalent to

$$M_{ik}^\top M_{ik} \preceq \tau^2 I, \quad \forall (i,k) \in \Omega_r \times \Omega_{r_e}.$$

Then, it follows from (37) that

$$M_{ik}^\top M_{ik} \preceq \varepsilon^2\mu^2 I \preceq \varepsilon^2 P^2. \tag{39}$$

Pre- and postmultiplying (39) with P^{-1}, it follows that

$$P^{-1} M_{ik}^\top M_{ik} P^{-1} \preceq \varepsilon^2 I,$$

which is equivalent to $\|K_{ik}\| \leq \varepsilon$.

Remark 7. An integral action can be easily introduced in the feedback control structure to improve the tracking performance. To this end, it suffices to include the integral state $\mathbf{x}_I(t)$, whose dynamics can be defined as

$$\dot{\mathbf{x}}_I(t) = C\mathbf{e}(t),$$

with $C = \begin{bmatrix} I & 0 \end{bmatrix} \in \mathbb{R}^{n\times 2n}$. This amounts substituting in the convex optimization problems A_i, B and E_k by the following respective partitioned matrices:

$$\begin{bmatrix} A_i & 0 \\ C & 0 \end{bmatrix}, \quad \begin{bmatrix} B \\ 0 \end{bmatrix}, \quad \begin{bmatrix} E_k & 0 \\ 0 & I \end{bmatrix}.$$

The following numerical experiments are obtained with the corresponding integral fuzzy feedback control scheme.

IV. Illustrative Results and Discussions

To highlight the interests of the proposed approach, we provides illustrative results obtained with the 2-DoF manipulator benchmark developed by ABB Robotics (Moberg et al. 2008). Then, objective comparisons with notable control approaches are also given.

A. Two Degree-of-Freedom Robot Manipulator

The studied manipulator is depicted in Fig. 1. The first arm rotates about the $z-$axis. The second arm is attached to the first arm by a revolute joint. The robot parameters are given in Table I. Let us denote $q_1(t)$ and $q_2(t)$ the relative joint coordinates of the first and the second arms, respectively, and $q_0(t) = q_1(t) + q_2(t)$ the absolute joint coordinate of the second arm. The torques at joints 1 and 2 are respectively denoted as $\Gamma_1(t)$ and $\Gamma_2(t)$. The manipulator dynamics can be expressed in the form (1) with $\mathcal{G}(\mathbf{q}) = \mathcal{P}(\mathbf{q})\mathbf{q}(t)$ and

$$\mathcal{M}(\mathbf{q}) = \begin{bmatrix} c_1 + 2c_2\cos q_2 + I_{a1} & c_3 + c_2\cos q_2 \\ c_3 + c_2\cos q_2 & c_3 + I_{a2} \end{bmatrix},$$

$$\mathcal{N}(\mathbf{q},\dot{\mathbf{q}}) = \begin{bmatrix} -2c_2\dot{q}_2\sin q_2 + f_{v1} & -c_2\dot{q}_2\sin q_2 \\ c_2\dot{q}_1\sin q_2 & f_{v2} \end{bmatrix},$$

$$\mathcal{P}(\mathbf{q}) = \begin{bmatrix} c_4\frac{\sin q_1}{q_1} + c_5\frac{\sin q_0}{q_0} & c_5\frac{\sin q_0}{q_0} \\ c_5\frac{\sin q_0}{q_0} & c_5\frac{\sin q_0}{q_0} \end{bmatrix},$$

TABLE I
MANIPULATOR NOMENCLATURE.

Symbol	Description	Value
L_1/L_2	Length of robot arms (m)	1/1.5
m_1/m_2	Mass of robot arms (kg)	50/150
I_1/I_2	Inertia of robot arms (kgm^2)	5/50
I_{a1}/I_{a2}	Inertia of actuator rotors (kgm^2)	160/40
r_1/r_2	Distance joints-mass centers (m)	0.5/ 0.8
f_{v1}/f_{v2}	Viscous friction coefficient (Nms/rd)	240/120
g	Gravitational acceleration (m/s^2)	9.81

where $c_1 = m_1 r_1^2 + I_1 + m_2 L_1^2 + m_2 r_2^2 + I_2$, $c_2 = m_2 L_1 r_2$, $c_3 = m_2 r_2^2 + I_2$, $c_4 = m_1 g r_1 + m_2 g L_1$, $c_5 = m_2 g r_2$. Let us define the state $\mathbf{x}(t) = \begin{bmatrix} q_1(t) & q_2(t) & \dot{q}_1(t) & \dot{q}_2(t) \end{bmatrix}^\top$, the control input $\Gamma(t) = \begin{bmatrix} \Gamma_1(t) & \Gamma_2(t) \end{bmatrix}^\top$. The disturbance input $\Gamma_d(t) = \begin{bmatrix} \Gamma_{d1}(t) & \Gamma_{d2}(t) \end{bmatrix}^\top$ is composed of the dry friction torques and the external forces as indicated in Appendix. The manipulator dynamics can be represented in the form (2) with

$$E(\mathbf{x}) = \begin{bmatrix} 1 & 0 & 0 & 0 \\ 0 & 1 & 0 & 0 \\ 0 & 0 & c_1 + 2c_2 z_1 & c_3 + c_2 z_1 \\ 0 & 0 & c_3 + c_2 z_1 & c_3 \end{bmatrix}, \quad B = \begin{bmatrix} 0 & 0 \\ 0 & 0 \\ 1 & 0 \\ 0 & 1 \end{bmatrix},$$

$$A(\mathbf{x}) = \begin{bmatrix} 0 & 0 & 1 & 0 \\ 0 & 0 & 0 & 1 \\ z_2 & z_3 & 2z_4 - f_{v1} & z_4 \\ z_3 & z_3 & z_5 & -f_{v2} \end{bmatrix},$$

where the premise variables are defined as follows:

$$\begin{aligned} &z_1 = \cos q_2, \quad z_4 = c_2 \dot{q}_2 \sin q_2, \quad z_5 = -c_2 \dot{q}_1 \sin q_2, \\ &z_2 = -c_4 \frac{\sin q_1}{q_1} - c_5 \frac{\sin q_0}{q_0}, \quad z_3 = -c_5 \frac{\sin q_0}{q_0}. \end{aligned} \tag{40}$$

B. Fuzzy Descriptor Modeling for Robot Tracking Control

The set $\mathscr{D}_x$ in (3) of the benchmark robot is defined with

$$\begin{aligned} &|q_1(t)| \leq \pi \text{ rad}, \qquad &&|q_2(t)| \leq \pi \text{ rad}, \\ &|\dot{q}_1(t)| \leq \pi/2 \text{ rad/s}, \quad &&|\dot{q}_2(t)| \leq \pi/2 \text{ rad/s}. \end{aligned}$$

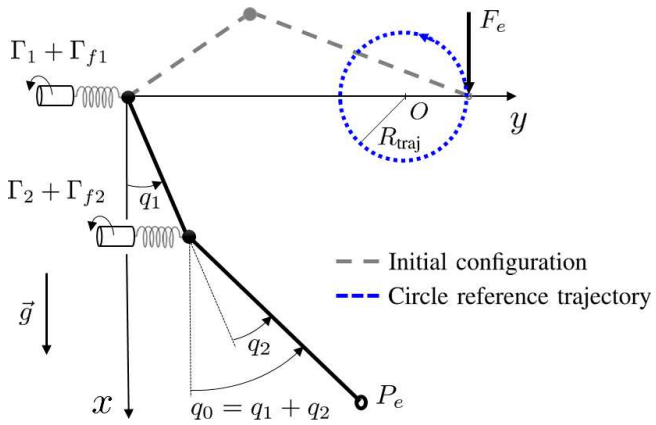

Fig. 1. Two degree-of-freedom benchmark manipulator.

These state limitations are determined to guarantee a large workspace together with the related physical robot constraints.

1) Exact Fuzzy Descriptor Model: From the physical parameters in Table I and the above workspace data, the bounds of the premise variables in (40) can be easily computed

$$\begin{aligned} z_{1\max} &= -z_{1\min} = 1, & z_{2\max} &= z_{3\max} = 255.7, \\ z_{2\min} &= -3384.5, & z_{3\min} &= -1177, \\ z_{4\max} &= -z_{4\min} = 188.5, & z_{5\max} &= -z_{5\min} = 188.5. \end{aligned}$$

Using the sector nonlinearity method shown in Section III-A, an *equivalent* fuzzy descriptor representation (10) with $2^5 = 32$ linear submodels ($r_e = 2$ and $r = 16$) of the studied manipulator, called $E-$Model, can be derived. The details of these 32 submodels and the corresponding MFs are standard and omitted here for brevity.

2) Reduced-Complexity Fuzzy Descriptor Model: For illustration, the premise variables z_i, $i \in \{2, 4, 5\}$, can be rewritten in the form (29). This leads to a fuzzy model (30) with $2^2 = 4$ linear submodels ($r^* = 2$ and $r_e^* = 2$), called $R-$Model. The state-space matrices of this fuzzy model are given by

$$\begin{aligned} E_1^* &= E(z_{1\min}), \quad E_2^* = E(z_{1\max}), \quad \Delta E_1(t) = \Delta E_2(t) = 0, \\ A_1^* &= \begin{bmatrix} 0 & 0 & 1 & 0 \\ 0 & 0 & 0 & 1 \\ z_{2m} & z_{3\min} & 2z_{4m} - f_{v1} & z_{4m} \\ z_{3\min} & z_{3\min} & z_{5m} & -f_{v2} \end{bmatrix}, \\ A_2^* &= \begin{bmatrix} 0 & 0 & 1 & 0 \\ 0 & 0 & 0 & 1 \\ z_{2m} & z_{3\min} & 2z_{4m} - f_{v1} & z_{4m} \\ z_{3\max} & z_{3\min} & z_{5m} & -f_{v2} \end{bmatrix}, \\ \Delta_a(t) &= \mathrm{diag}(\delta_2(t), \delta_4(t), \delta_5(t)), \\ H_a &= \begin{bmatrix} 0 & 0 & 1 & 0 \\ 0 & 0 & 1 & 0 \\ 0 & 0 & 0 & 1 \end{bmatrix}^\top, \quad W_a = \begin{bmatrix} z_{2r} & 0 & 0 & 0 \\ 0 & 0 & 2z_{4r} & z_{4r} \\ 0 & 0 & z_{5r} & 0 \end{bmatrix}. \end{aligned}$$

The corresponding MFs of $R-$Model are given by

$$\begin{aligned} v_1(\mathbf{z}) &= \frac{z_1 - z_{1\min}}{z_{1\max} - z_{1\min}}, \quad v_2(\mathbf{z}) = 1 - v_1(\mathbf{z}), \\ h_1(\mathbf{z}) &= \frac{z_3 - z_{3\min}}{z_{3\max} - z_{3\min}}, \quad h_2(\mathbf{z}) = 1 - h_1(\mathbf{z}). \end{aligned}$$

The control results obtained with the two above manipulator fuzzy models are discussed below.

C. Numerical Results and Discussions

Solving directly the optimization problems in Theorems 1 and 2 with a decay rate $\alpha = 15$ yields *impractical* control laws (14) or (31) with a gain-amplitude order of 10^9. We thus redesign the control gains by including additional LMI constraints as explained in Remark 6 to guarantee that $\|K_{ik}\| \leq 10^6$, for $\forall (i,k) \in \Omega_r \times \Omega_{r_e}$. Details on the obtained control solutions are not given here for brevity. A summary on the control design of both manipulator fuzzy models is depicted in Table II. Remark that using relation (29), the number of linear subsystems of the fuzzy descriptor representation is significantly reduced from 32 to 4. This leads to a major advantage for real-time control implementation without fear of causing closed-loop instability since Theorem 2 allows designing a robust controller (31) with respect to uncertainties $\Delta_a(t)$ and $\Delta_e(t)$, induced by the complexity reduction. Moreover, the number of scalar decision variables $\mathcal{N}_{var}$ involved in LMI-based optimizations, representing their numerical complexity, is also drastically reduced for the control of $R-$Model. The $\mathcal{L}_\infty-$gain γ obtained for both fuzzy models are very small, thus, a good level of tracking performance is expected for both control solutions. Note that no feasible solution can be found for any manipulator fuzzy representation with less than four linear submodels since the uncertainties caused by

(29) become too large. Hence, in practice there is a tradeoff between numerical complexity reduction and modeling uncertainty as mentioned in Remark 3.

TABLE II
CONTROL DESIGN OF TWO FUZZY DESCRIPTOR MODELS.

Fuzzy model	Nb. submodels	Design	$\mathcal{N}_{var}$	γ
$E-$Model	32	Theorem 1	1562	8.06×10^{-5}
$R-$Model	4	Theorem 2	222	7.75×10^{-6}

The numerical experiments are performed with a refined robot model that takes into account the joint elasticity and dry friction effect, see Appendix. This high-fidelity simulation model is embedded in Simscape Multibody$^{\text{TM}}$ environment. The trajectory reference in the Cartesian space is a circle with radius $R_{\text{traj}} = 0.4$ (m) and center coordinates $O(0, 1.8)$ (m), which has to be performed in 3.2 (s) with a quintic polynomial of time. The joint trajectory is computed using manipulator inverse kinematics from the Cartesian trajectory. We now compare the tracking performance obtained with the following four controllers:

- LI32 controller is derived from Theorem 1 and E-Model,
- LI4 controller is derived from Theorem 2 and R-Model,
- PID controller and CTC controller, whose structures and design tunings have been chosen according to (Paccot et al. 2009).

The relative circularity errors $\epsilon_c = \frac{\|OP_e(t)\| - R_{\text{traj}}}{R_{\text{traj}}}$, where $P_e(t)$ is the tool center point (TCP), obtained with the four controllers are depicted in Fig. 2. Observe that both proposed LI32 and LI4 controllers provide a high-precision tracking performance with respect to the considered trajectory reference. In particular, despite its reduced-complexity feature, controller LI4 offers similar, or even better, control performance compared to the other ones. These facts are also confirmed by the small tracking errors obtained with both proposed controllers as indicated in Fig. 3.

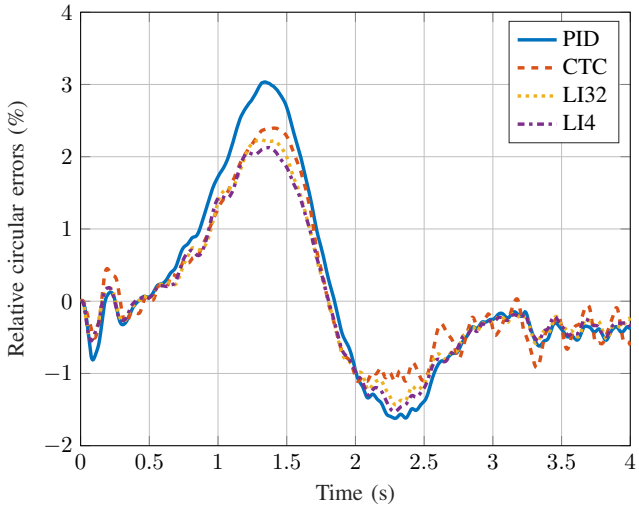

Fig. 2. Time history of the relative circularity errors ϵ_c for the four compared controllers PID, CTC, LI32 and LI4.

To further illustrate the tracking performance of different controllers, let us consider the following performance indices:

- $\Delta R_M = \max\limits_{t\in[0,T]} \|OP_e(t)\| - R_{\text{traj}}$ (mm): maximal circular error, where $T = 4$ (s) is the simulation duration,
- $\Delta e_{x,M}$ and $\Delta e_{y,M}$ (mm): tracking errors with respect to the tool center point $P_e(t)$ in x and y directions,
- $E_{i\text{MaAV}}$ (mrad): maximum absolute value (MaAV) of the ith joint position tracking error, defined by

$$E_{i\text{MaAV}} = \max_{t\in[0,T]} |q_i(t) - q_{ir}(t)|, \quad i = 1, 2.$$

Fig. 4 represents the values of these performance indices obtained with the considered controllers. This chart corroborates the good performance obtained by the proposed control laws compared with existing controllers. Especially, the tradeoff between the controller complexity and the related performance is also clarified. The simplest PID controller provides the worst values for all considered performance indices whereas more complex control schemes such as CTC or LI32 yield better tracking performance. The proposed controller LI4 appears as a good compromise leading to a simple enough control structure for real-time validation without any significant degradation of tracking performance.

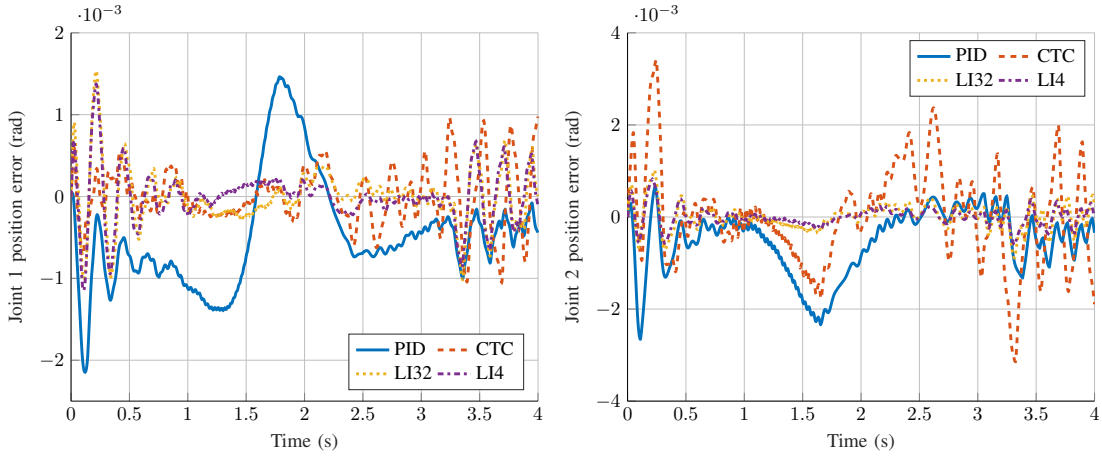

Fig. 3. Time history of the joint position errors.

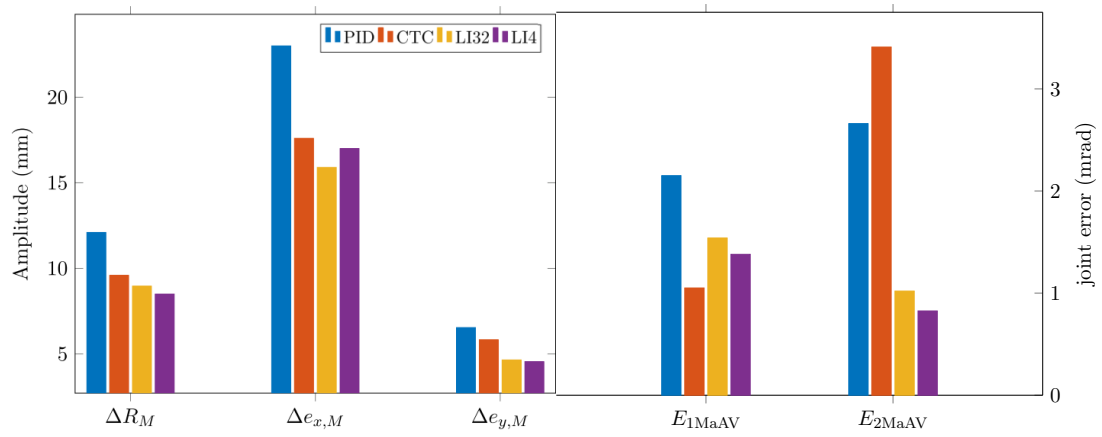

Fig. 4. Comparison of tracking control performance indices.

Concerning the actuator solicitations, Fig. 5 depicts the corresponding response of both control torques. Moreover, Table III shows the maximal and the root-mean-square (RMS) values of the two actuator torques of the benchmark manipulator. We can observe that all the torque values are of similar magnitudes for the four considered controllers.

TABLE III
MAXIMAL AND RMS ACTUATOR TORQUES AFTER GEARBOX (IN NM) FOR DIFFERENT CONTROLLERS.

Controller	$\Gamma_{1\mathrm{max}}$	$\Gamma_{1\mathrm{RMS}}$	$\Gamma_{2\mathrm{max}}$	$\Gamma_{2\mathrm{RMS}}$
PID	4804	1282	2165	476.3
CTC	4484	1273	2103	463.2
LI32	4478	1275	2131	471.1
LI4	4709	1279	2138	473.6

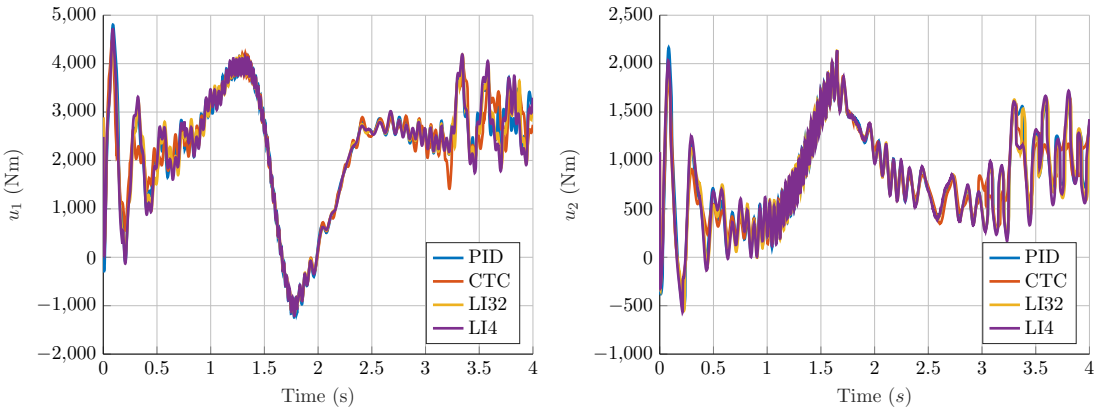

Fig. 5. Time history of the control torques.

V. Concluding Remarks

A systematic approach for tracking control design of robot manipulators has been proposed. Based on a fuzzy descriptor representation of generic manipulator systems, this approach makes use of Lyapunov stability arguments to guarantee an $\mathcal{L}_\infty-$gain performance of the closed-loop tracking error dynamics. Exploiting a robust control scheme, we propose an effective way to significantly reduce the numerical complexity of the control structure, leading to a major advantage for real-time control implementation. The control design is recast as convex optimization problems, which can be easily solved with standard solvers. The practical tracking performance of the proposed approach is clearly demonstrated with a high-fidelity 2-DoF benchmark manipulator. A comparative study with several prominent tracking control schemes is also performed to show the interests of the new approach. In particular, it has been shown that despite a significant complexity reduction, the robust fuzzy controller provides a similar tracking performance compared to the exact fuzzy controller. Hence, the proposed robust fuzzy-model-based control method offers a more effective solution for the tracking control problem of robot manipulators, especially within industrial context. Future works focus on the extension of the proposed approach to the design of a robust fuzzy output tracking control for robot manipulators and real-time validations. Moreover, fuzzy robot tracking control in interaction with human operators is also a promising research topic.

Appendix. Manipulator Benchmark Model

The dynamics of the rigid-link flexible-joint manipulator model used for validation purposes is composed of actuator dynamics (subscript a) and linkage dynamics (subscript b) as

$$\begin{aligned} &\mathcal{M}_a\ddot{\mathbf{q}}_a + \mathcal{N}_a\dot{\mathbf{q}}_a + \mathscr{Q}_t = \Gamma + \Gamma_f \\ &\mathcal{M}_b(\mathbf{q}_b)\ddot{\mathbf{q}}_b + \mathcal{N}_b(\mathbf{q}_b,\dot{\mathbf{q}}_b)\dot{\mathbf{q}}_b + \mathcal{G}(\mathbf{q}_b) - \mathscr{Q}_t = \mathcal{J}^\top(\mathbf{q}_b)F_e, \end{aligned} \tag{41}$$

where $\mathscr{Q}_t = \mathcal{B}_t(\dot{\mathbf{q}}_a - \dot{\mathbf{q}}_b) + \mathcal{K}_t(\mathbf{q}_a - \mathbf{q}_b)$, $\mathbf{q}_a = \begin{bmatrix} q_{a1} & q_{a2} \end{bmatrix}^\top$ is the vector of actuator angular positions, $\mathcal{M}_a = \mathrm{diag}(I_{a1}, I_{a2})$ is the matrix of motor inertia, $\mathcal{N}_a = \mathrm{diag}(f_{v1}, f_{v2})$ is the matrix of viscous friction, $\mathcal{M}_b(\mathbf{q}_b)$ and $\mathcal{N}_b(\mathbf{q}_b, \dot{\mathbf{q}}_b)$ are respectively the linkage inertia and Coriolis/centripetal matrices, $\mathcal{K}_t = \mathrm{diag}(k_{t1}, k_{t2})$ is the matrix of joint stiffness, $\mathcal{B}_t = \mathrm{diag}(b_{t1}, b_{t2})$ is the joint damping matrix, and $\mathcal{J}(\mathbf{q}_b)$ is the robot Jacobian such that the TCP velocity is expressed as $\dot{\mathbf{X}}_{P_e}(t) = \mathcal{J}(\mathbf{q}_b)\dot{\mathbf{q}}_b(t)$. The disturbances are composed of the dry friction torque $\Gamma_f(t)$ acting on the actuators and the external force $F_e(t)$ acting on the TCP. The dry friction torque $\Gamma_f(t) = \begin{bmatrix} \Gamma_{f1}(t) & \Gamma_{f2}(t) \end{bmatrix}^\top$ is modeled as follows (Moberg et al. 2008):

$$\Gamma_{fi}(t) = \Gamma_{ci}(\mu_i + (1-\mu_i)\cosh^{-1}(\beta_i\dot{q}_{ai}(t)))\tanh(\alpha_i\dot{q}_{ai}(t)),$$

where Γ_{ci} is the Coulomb friction, μ_i is the Stribeck friction constant, and α_i, β_i are the constants of the smooth friction model for the ith joint. The external force used for validation is assumed to be tangential to the TCP trajectory as

$$F_e(t) = f_e(t)\dot{\mathbf{X}}_{P_e}(t)\|\dot{\mathbf{X}}_{P_e}(t)\|^{-1},$$

where $f_e(t) \in \left[310, 490\right]$ (N) is the force magnitude. All the robot parameters are taken from the experimental benchmark (Moberg et al. 2008) of an industrial manipulator developed by ABB Robotics.

Note that the manipulator model (41) has four degrees-of-freedom, including the joint deformation between each actuator and its corresponding arm (Makarov et al. 2016). This additional and weakly damped dynamics introduces vibrations due to the excitation of the mechanical resonances. For control design, the joints are assumed to be rigid, *i.e.*, $\mathbf{q}_a = \mathbf{q}_b = \mathbf{q}$. This leads to the control-based manipulator model with matrices $\mathcal{M}(\mathbf{q}) = \mathcal{M}_a + \mathcal{M}_b(\mathbf{q})$, $\mathcal{N}(\mathbf{q}, \dot{\mathbf{q}}) = \mathcal{N}_a + \mathcal{N}_b(\mathbf{q}, \dot{\mathbf{q}})$, $\mathcal{G}(\mathbf{q})$ given in Section IV-A. Moreover, the disturbance input is defined as $\Gamma_d(t) = \mathcal{J}^\top(\mathbf{q}) F_e(t) + \Gamma_f(t)$.

Conflict of Interest. The authors declare that they have no conflict of interest.

REFERENCES

Arteaga-Pérez, M. A. (2019), 'An alternative proof to the asymptotic stability of PID controllers for regulation of robot manipulators', *IFAC J. Syst. Control* **9**, 100066.

Baek, J., Jin, M. & Han, S. (2016), 'A new adaptive sliding-mode control scheme for application to robot manipulators', *IEEE Trans. Indus. Electron.* **63**(6), 3628–3637.

Boyd, S., El Ghaoui, L., Feron, E. & Balakrishnan, V. (1994), *Linear Matrix Inequalities in System and Control Theory*, SIAM, Philadelphia.

Buondonno, G. & De Luca, A. (2016), 'Efficient computation of inverse dynamics and feedback linearization for VSA-based robots', *IEEE Rob. Autom. Lett.* **1**(2), 908–915.

Chen, B., Liu, X. & Tong, S. (2007), 'Adaptive fuzzy output tracking control of MIMO nonlinear uncertain systems', *IEEE Trans. Fuzzy Syst.* **15**(2), 287–300.

Dawson, D., Abdallah, C. & Lewis, F. (2003), *Robot Manipulator Control: Theory and Practice*, CRC Press.

de Jesús Rubio, J. (2017), 'Sliding mode control of robotic arms with deadzone', *IET Control Theory Appl.* **11**(8), 1214–1221.

Gaidhane, P., Nigam, M., Kumar, A. & Pradhan, P. (2019), 'Design of interval type-2 fuzzy precompensated PID controller applied to two-DoF robotic manipulator with variable payload', *ISA Trans.* **89**, 69–85.

He, X., He, W., Qin, H. & Sun, C. (2018), 'Boundary vibration control for a flexible Timoshenko robotic manipulator', *IET Control Theory Appl.* **12**(7), 875–882.

Jafarov, E., Parlakci, A. & Istefanopulos, Y. (2005), 'A new variable structure PID-controller design for robot manipulators', *IEEE Trans. Control Syst. Technol.* **13**(1), 122–130.

Jia, X., Zhang, D., Hao, X. & Zheng, N. (2009), 'Fuzzy $\mathcal{H}_\infty$ tracking control for nonlinear networked control systems in T–S fuzzy model', *IEEE Trans. Syst., Man, Cybern., Part B* **39**(4), 1073–1079.

Jin, L., Li, S., Yu, J. & He, J. (2018), 'Robot manipulator control using neural networks: A survey', *Neurocomputing* **285**, 23–34.

Jonnalagadda, K., Elumalai, K., Singh, H. & Prasad, A. (2020), 'Nonlinear control design using Takagi-Sugeno fuzzy applied to under-actuated visual servo system', *Trans. Inst. Meas. Control* p. 0142331220936584.

Li, H., Wu, C., Jing, X. & Wu, L. (2017), 'Fuzzy tracking control for nonlinear networked systems', *IEEE Trans. Cybern.* **7**(8), 20–31.

Li, Z. & Huang, D. (2020), 'Robust control of two-link manipulator with disturbance torque and time-varying mass loads', *Trans. Inst. Meas. Control* p. 0142331219894413.

Löfberg, J. (2004), YALMIP: A toolbox for modeling and optimization in Matlab, *in* 'IEEE Int. Symp. Comput. Aided Control Syst. Des.', Taipei, pp. 284–289.

Makarov, M., Grossard, M., Rodríguez, P. & Dumur, D. (2016), 'Modeling and preview $\mathcal{H}_\infty$ design for motion control of elastic-joint robots with uncertainties', *IEEE Trans. Ind. Electron.* **3**(10), 9–38.

Marwan, A., Farrukh, N., Sahari, M. & Hanim, S. (2013), 'Real-time on line tuning of fuzzy controller for two-link rigid–flexible robot manipulators', *Trans. Inst. Meas. Control* **35**(6), 730–741.

Meng, Y., Yang, H. & Jiang, B. (2020), 'Multi-model switching-based fault tolerant control for planar robot manipulators', *IET Control Theory Appl.* **14**, 1–11.

Moberg, S., Öhr, J. & Gunnarsson, S. (2008), 'A benchmark problem for robust control of a multivariable nonlinear flexible manipulator', *IFAC Proc. Volume* **41**(2), 1206–1211.

Nasiri, N., Fakharian, A. & Menhaj, M. B. (2020), 'Observer-based robust control for flexible-joint robot manipulators: A state-dependent Riccati equation-based approach', *Trans. Inst. Meas. Control* p. 0142331220941653.

Nguyen, A.-T., Coutinho, P., Guerra, T., Palhares, R. & Pan, J. (2020), 'Constrained output-feedback control for discrete-time fuzzy systems with local nonlinear models subject to state and input constraints', *IEEE Trans. Cybern.* pp. 1–12. DOI: 10.1109/TCYB.2020.3009128.

Nguyen, A.-T., Guerra, T.-M., Sentouh, C. & Zhang, H. (2019), 'Unknown input observers for simultaneous estimation of vehicle dynamics and driver torque: Theoretical design and hardware experiments', *IEEE/ASME Trans. Mechatron.* **24**(6), 2508–2518.

Nguyen, A.-T., Pan, J., Guerra, T.-M. & Wang, Z. (2021), 'Avoiding unmeasured premise variables in designing unknown input observers for Takagi–Sugeno fuzzy systems', *IEEE Control Syst. Lett.* **5**(1), 79–84.

Nguyen, A.-T., Rath, J., Guerra, T.-M., Palhares, R. & Zhang, H. (2020), 'Robust set-invariance based fuzzy output tracking control for vehicle autonomous driving under uncertain lateral forces and steering constraints', *IEEE Trans. Intell. Transp. Syst.* pp. 1–12. DOI: 10.1109/TITS.2020.3021292.

Nguyen, A.-T., Taniguchi, T., Eciolaza, L., Campos, V., Palhares, R. & Sugeno, M. (2019), 'Fuzzy control systems: Past, present and future', *IEEE Comput. Intell. Mag.* **14**(1), 56–68.

Nguyen, V.-A., Nguyen, A.-T., Dequidt, A., Vermeiren, L. & Dambrine, M. (2019), 'Nonlinear tracking control with reduced complexity of serial robots: A robust fuzzy descriptor approach', *Int. J. Fuzzy Syst.* **21**(4), 1038–1050.

Nojavanzadeh, D. & Badamchizadeh, M. (2016), 'Adaptive fractional-order non-singular fast terminal sliding mode control for robot manipulators', *IET Control Theory Appl.* **10**(13), 1565–1572.

Ouyang, Y., He, W. & Li, X. (2017), 'Reinforcement learning control of a single-link flexible robotic manipulator', *IET Control Theory Appl.* **11**(9), 1426–1433.

Paccot, F., Andreff, N. & Martinet, P. (2009), 'A review on the dynamic control of parallel kinematic machines: Theory and experiments', *Int. J. Robotics Res.* **28**(3), 395–416.

Pan, J., Nguyen, A.-T., Guerra, T.-M. & Ichalal, D. (2020), 'A unified framework for asymptotic observer design of fuzzy systems with unmeasurable premise variables', *IEEE Trans. Fuzzy Syst.* pp. 1–1. DOI: 10.1109/TFUZZ.2020.3009737.

Pan, Y., Li, X. & Yu, H. (2019), 'Efficient PID tracking control of robotic manipulators driven by compliant actuators', *IEEE Trans. Control Syst. Technol.* **27**(2), 915–922.

Sahu, U. K., Subudhi, B. & Patra, D. (2019), 'Sampled-data extended state observer-based backstepping control of two-link flexible manipulator', *Trans. Inst. Meas. Control* **41**(13), 3581–3599.

Song, Z., Yi, J., Zhao, D. & Li, X. (2005), 'A computed torque controller for uncertain robotic manipulator systems: Fuzzy approach', *Fuzzy Sets Syst.* **154**(2), 208–226.

Sun, W., Su, S., Xia, J. & Nguyen, V. (2019), 'Adaptive fuzzy tracking control of flexible-joint robots with full-state constraints', *IEEE Trans. Syst., Man, Cybern.: Syst.* **49**(11), 2201–2209.

Sun, Z., Zhang, Y., Li, S. & Zhang, X. (2019), 'Decentralized robust tracking control for 2-degree of freedom planar robot manipulator subject to disturbances and uncertainties', *Trans. Inst. Meas. Control* **41**(14), 3909–3920.

Tanaka, K. & Wang, H. O. (2004), *Fuzzy Control Systems Design and Analysis: A Linear Matrix Inequality Approach*, John Wiley & Sons.

Taniguchi, T., Tanaka, K. & Wang, H. (2000), 'Fuzzy descriptor systems and nonlinear model following control', *IEEE Trans. Fuzzy Syst.* **8**(4), 442–452.

Tseng, C.-S., Chen, B.-S. & Uang, H.-J. (2001), 'Fuzzy tracking control design for nonlinear dynamic systems via T-S fuzzy model', *IEEE Trans. Fuzzy Syst.* **9**(3), 381–392.

Van, M., Ge, S. & Ren, H. (2016), 'Finite time fault tolerant control for robot manipulators using time delay estimation and continuous nonsingular fast terminal sliding mode control', *IEEE Trans. Cybern.* **47**(7), 1681–1693.

Vermeiren, L., Dequidt, A., Afroun, M. & Guerra, T.-M. (2012), 'Motion control of planar parallel robot using the fuzzy descriptor system approach', *ISA Trans.* **51**(5), 596–608.

Wang, T., Qiu, J., Yin, S., Gao, H., Fan, J. & Chai, T. (2016), 'Performance-based adaptive fuzzy tracking control for networked industrial processes', *IEEE Trans. Cybern.* **46**(8), 1760–1770.

Yang, C., Jiang, Y., He, W., Na, J., Li, Z. & Xu, B. (2018), 'Adaptive parameter estimation and control design for manipulators with finite-time convergence', *IEEE Trans. Indus. Electron.* **6**(10), 12–23.

Zhang, H., Shi, Y. & Liu, M. (2013), '$\mathcal{H}_\infty$ step tracking control for networked discrete-time nonlinear systems with integral and predictive actions', *IEEE Trans. Indus. Inform.* **9**(1), 337–345.

Zhang, L., Liu, L., Wang, Z. & Xia, Y. (2018), 'Continuous finite-time control for uncertain robot manipulators with integral sliding mode', *IET Control Theory Appl.* **12**(11), 1621–1627.

Zhang, S., Dong, Y., Ouyang, Y., Yin, Z. & Peng, K. (2018), 'Adaptive neural control for robotic manipulators with output constraints and uncertainties', *IEEE Trans. Neural Netw. Learn. Syst.* **29**(11), 5554–5564.

Zhang, S., Lei, M., Dong, Y. & He, W. (2016), 'Adaptive neural network control of coordinated robotic manipulators with output constraint', *IET Control Theory Appl.* **10**(17), 2271–2278.

Zhang, Y., Chen, S., Li, S. & Zhang, Z. (2017), 'Adaptive projection neural network for kinematic control of redundant manipulators with unknown physical parameters', *IEEE Trans. Indus. Electron.* **65**(6), 4909–4920.

Zhang, Z., Zheng, L., Yu, J., Li, Y. & Yu, Z. (2017), 'Three recurrent neural networks and three numerical methods for solving a repetitive motion planning scheme of redundant robot manipulators', *IEEE/ASME Trans. Mechatron.* **22**(3), 1423–1434.

Zhou, Q., Shi, P., Lu, J. & Xu, S. (2011), 'Adaptive output-feedback fuzzy tracking control for a class of nonlinear systems', *IEEE Trans. Fuzzy Syst.* **19**(5), 972–982.